PLASMA DYNAMICS

Prof. S. C. Brown	E. V. George	J. J. McCarthy
Prof. W. P. Allis	W. H. Glenn, Jr.	W. J. Mulligan
Prof. G. Bekefi	E. B. Hooper, Jr.	J. J. Nolan, Jr.
Prof. D. R. Whitehouse	P. W. Jameson	L. D. Pleasance
Dr. G. Lampis	A. N. Kramer	G. L. Rogoff
M. L. Andrews	R. L. Kronquist	D. W. Swain
J. K. Domen	D. T. Llewellyn-Jones	F. Y-F. Tse
D. L. Flannery	E. M. Mattison	R. E. Zelazo

A. ELECTRON DENSITY MEASUREMENTS WITH A LASER INTERFEROMETER

A laser interferometer to measure small dielectric coefficients has been described in a previous report.[1] In the interferometer three mirrors are placed in a straight line to form two coupled optical cavities, one containing the laser plasma and the other the dielectric that is to be studied. In the present case this is a plasma. The laser itself then acts as a detector for the unknown dielectric coefficient.[2]

The present system uses a compensation technique to study repetitively pulsed plasmas. A calibrated variable dielectric is placed in series with the unknown and adjusted to balance it. Because the plasma is pulsed, a null technique is used in which the cavity containing the two dielectrics is compared with the "empty" cavity. In this
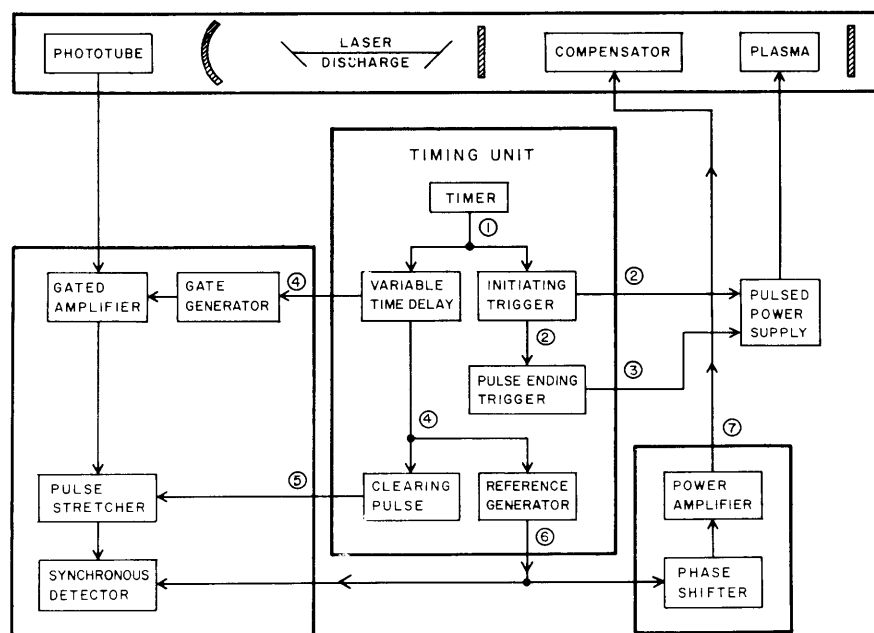

Fig. IX-1. Schematic diagram of the experiment.

manner, dielectric coefficients have been measured with uncertainties of approximately $10^{-3}/L\lambda$, where L is the length of the dielectric in centimeters, and λ the laser wavelength in microns. For studies of a plasma with the 3.39 μ line of the helium-neon laser used this corresponds to an electron density of approximately $(10^{13}/L)$ cm^{-3}.

The output of the laser is detected by a photomultiplier that drives a gated amplifier. The use of the gated amplifier permits a determination of the time dependence of the electron density of the plasma. In such a manner, plasmas that decay at the exponential rate of a few microseconds can be studied. As the noise that is present in the interferometer arises primarily from vibrations and from sound in the room, and hence falls off rapidly at high frequencies, the sensitivity of the gated instrument is almost that of the ungated system.

A block diagram of the electronic system is shown in Fig. IX-1. The timing circuits are essentially the same as those used in the afterglow microwave radiometer, to which the reader is referred for details.[3]

The compensator has been changed from the crystalline quartz previously described.[1] The compensator employing the electro-optic effect in quartz was discarded for two reasons: very high voltages were required for reasonable phase shifts, and acoustic waves were generated in the quartz by these voltages which led to nonreproducible results. The present compensator utilizes an acoustic driver to produce a sound wave travelling across the beam. The varying density of air then produces a phase shift in the light.

The compensator was calibrated by using the multiple-pass technique of Gerardo and Verdeyden[4] and was measured to be linear to within 2 per cent. We had some difficulty with pick-up of acoustic waves by the laser, but this effect was reduced to accepted limits by careful shielding. It was found that if the laser discharge contained striations, they tended to "lock-on" to changes in the laser light intensity. To prevent such striations the laser was operated with both DC current and an RF (30-Mc) voltage applied by means of metal strips around the discharge tube.

The discharge which is being studied at present with the interferometer is a pulsed P.I.G. discharge. The discharge is shown in Fig. IX-2. The current pulses are of approximately 150 amps at 200 volts and of 75-μsec length (see Fig. IX-5). The gas pressure is in the range of 0.010-0.200 torr, and the magnetic field varied from 0-800 gauss.

The laser intensity as a function of time is shown in Fig. IX-3. Here the slowly varying signal is due to the compensator, and the rapidly varying signal to the plasma. The gated amplifier samples this signal twice during each cycle, once during the plasma pulse, and once at the peak of the compensator signal.

An expanded picture of the laser intensity during the plasma pulse is shown in Fig. IX-4. The electron density as measured by the interferometer is shown in Fig. IX-5.
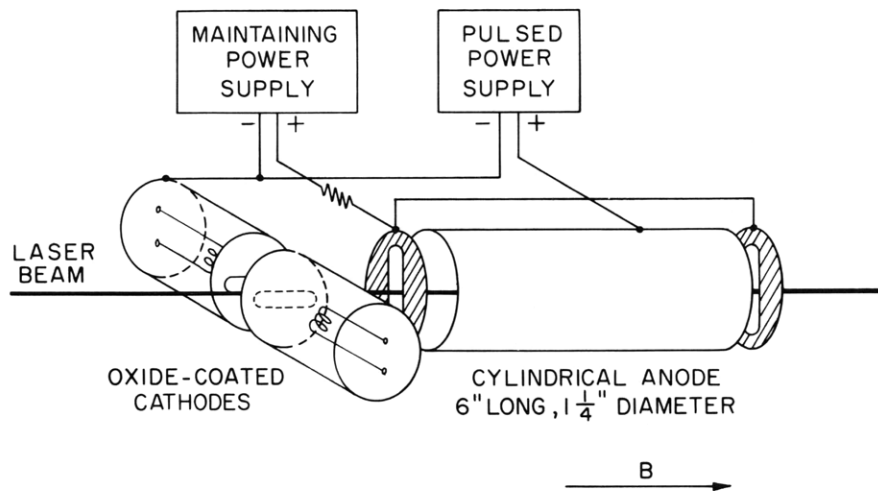
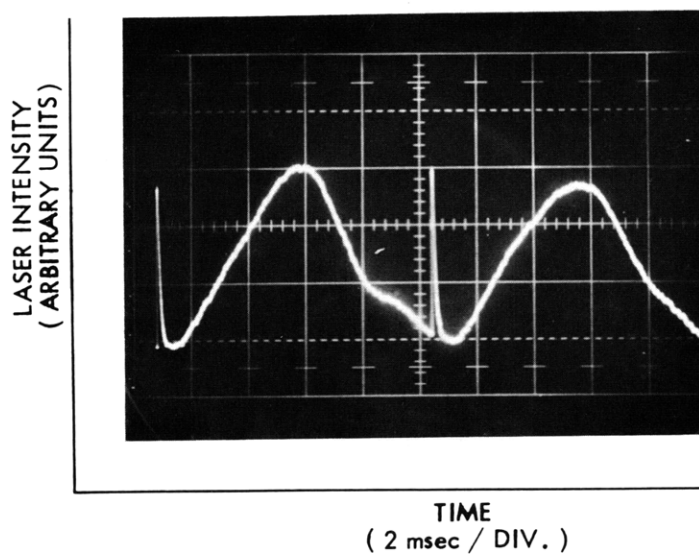Fig. IX-2. P.I.G. discharge.
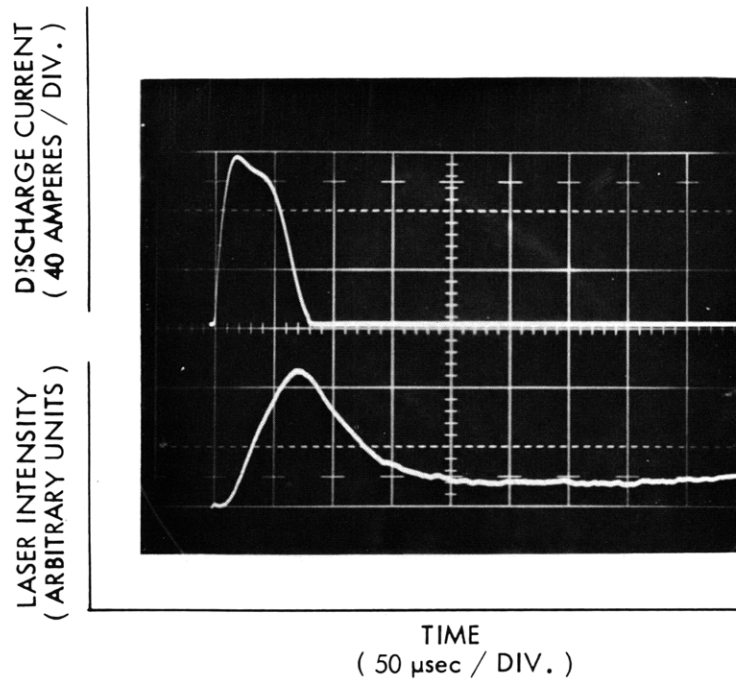

Fig. IX-3. Laser intensity.
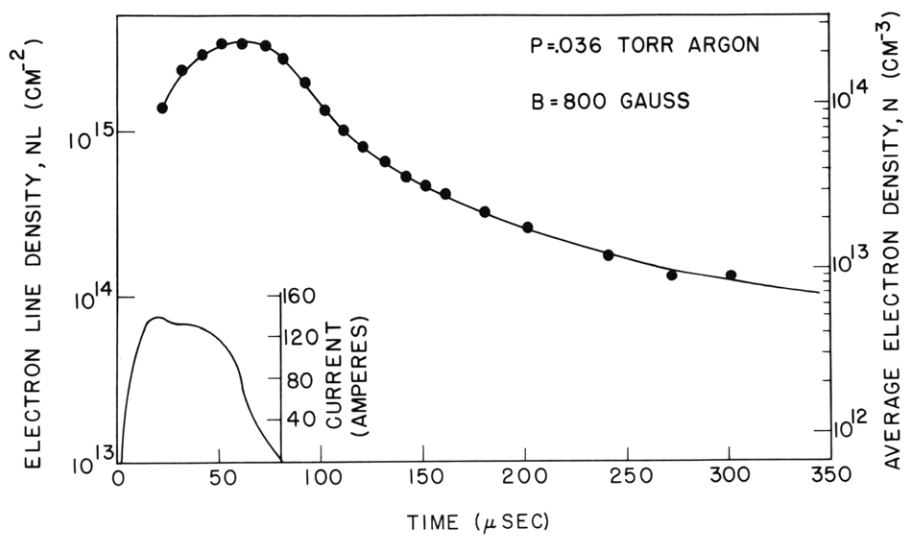
Fig. IX-4. Discharge current and laser intensity.

Fig. IX-5. Electron density in the plasma.

The decay of the plasma is now being studied in detail. The results thus far indicate that the decay can be explained entirely on the basis of ambipolar diffusion, if the electrons are assumed to have temperatures of several electron volts and the ions to have temperatures of almost 1 volt. This model is in accord with previous measurements made during the pulse on low-pressure P.I.G. discharges.[5] Although there is some evidence of instabilities during the current pulse, there is no present indication that instabilities affect the decay of the plasma.

E. B. Hooper, Jr.

References

1. E. B. Hooper, Jr., "Laser Interferometer," Quarterly Progress Report No. 75, Research Laboratory of Electronics, M.I.T., October 15, 1964, p. 55.

2. D. E. T. F. Ashby and D. F. Jephcott, Appl. Phys. Letters 3, 13 (1963).

3. J. C. Ingraham and J. J. McCarthy, Quarterly Progress Report No. 64, Research Laboratory of Electronics, M.I.T., January 15, 1962, pp. 76-79.

4. J. B. Gerardo and J. T. Verdeyden, Appl. Phys. Letters 3, 121 (1963).

5. R. Geller and D. Pigache, "Plasma Physics," J. Nucl. Energy, Part C 4, 229 (1962).

B. REVERSAL OF ROTATION AND STEADY-STATE CHARACTERISTICS OF A BEAM-PLASMA DISCHARGE

A preliminary report[1] has been given on a rotation observed in a discharge initiated by an 800-volt electron gun (oxide-coated cathode, VA-220) with an output of
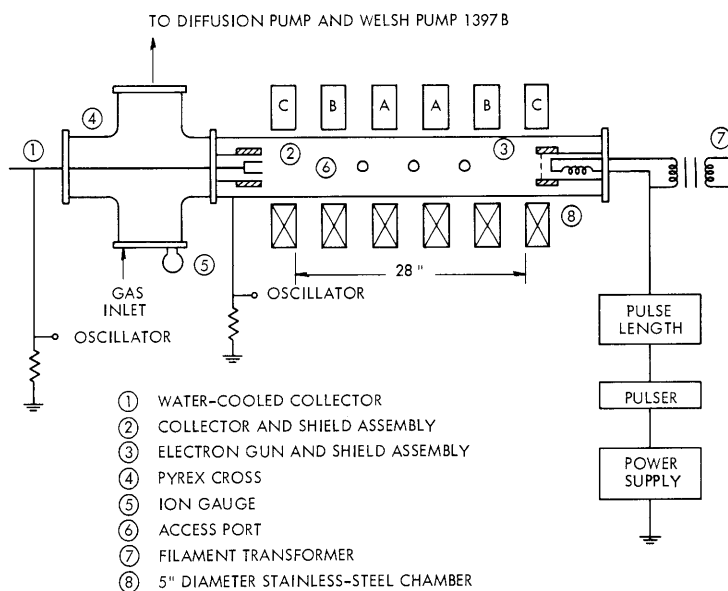

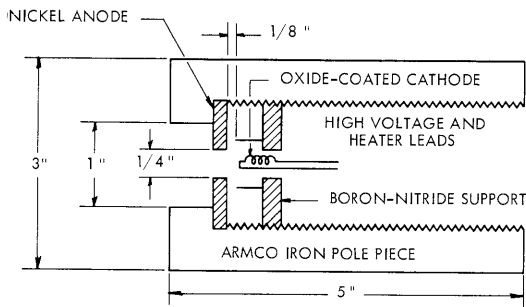Fig. IX-6. Beam plasma general arrangement.

Fig. IX-7. Detail of electron gun assembly.

approximately 20 ma, operated at pulsed lengths of a few milliseconds to achieve a steady state, or on DC.[1] The general characteristics of the initiation of this type of plasma have been described by Getty and Smullin.[2]

1. Apparatus

Schematic diagrams of the apparatus are shown in Figs. IX-6 and IX-7. The plasma is produced by electrons drifting through a region, 28 inches long, between an electron collector and a Pierce gun with an anode-cathode separation of 1/8 inch. Symmetrical Armco iron pole pieces, 3 inches in diameter, form magnetic shields for the hollow-cylinder and electron gun. The entire system is enclosed in a stainless-steel chamber, 5 inches in diameter. Low-value resistors detect current flow to various regions of the system, so essentially the entire assembly is at anode potential. The discharge is operated in an argon atmosphere, generally at a pressure of 10^{-4} mm, and the argon is pumped continuously across one of the ends of the chamber. A solenoid system of 6 coils energized by 3 regulated power supplies permits radial access into the chamber, and produces high mirror ratios, yet maintains a uniform field that is more than 1 ft long in the central region with a 1-2 per cent decrease off axis, although a uniform field was not always needed for the rotation.

2. Reversal of Rotation and Flute Modes

Plasma rotation with mode perturbations has been observed in a wide variety of plasmas.[3] A reversal of rotation is reported in a slow magnetic compression where the column rotates in the m = 1 mode. Left-handed rotation occurs when a "hot-ion" plasma is present, but then becomes right-handed as compression continues.[4]

The present weakly ionized plasma (less than 1 per cent), characterized by a dominant m = 2 flute mode, rotates in a left-handed sense in the range ≈ 80-≈ 200 gauss, with the frequency decreasing from 5 kc/sec. After the stoppage of rotation near a critical field of 200 gauss, the rotation becomes right-handed, attaining an asymptotic value of 3 kc/sec at high fields (1000 gauss). The m = 4 mode appears intermittently in the right-handed region until a few hundred gauss is attained. The typical dependence of the frequency of rotation on the central field for a fixed mirror ratio is shown by the heavy line in Fig. IX-8, with the lighter lines indicating the ranges in which the m = 2 and m = 4 modes appear. Though not indicated in the figure, the field was extended to 1500 gauss, with the frequency remaining at the asymptotic value of 3 kc/sec. At the crossover point, the electron cyclotron frequency corresponded to the plasma frequency with an accuracy
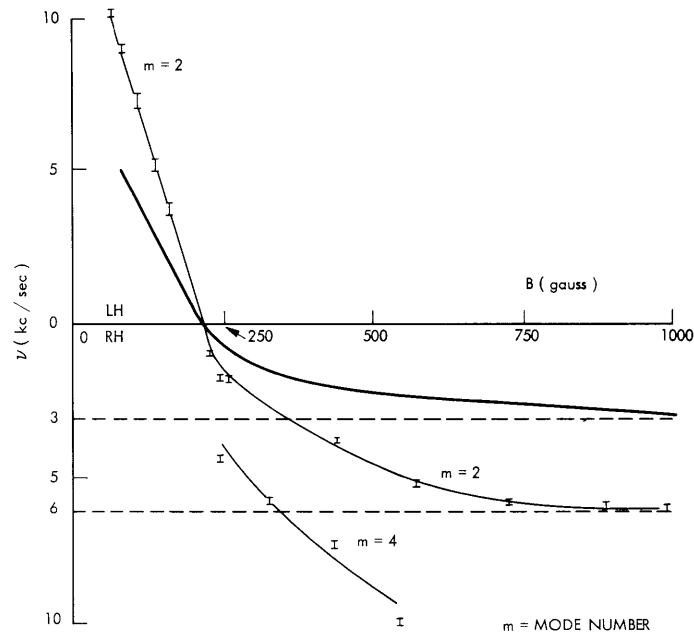
Fig. IX-8. Frequency and mode dependence of rotation on central magnetic field. Mirror ratio, 2.2; gun voltage, 820; pressure, 1.2×10^{-4} mm; crossover, ≈ 200 gauss. At crossover, $\nu_p \approx \nu_{ec} = 550$ Mc/sec.

of measuremeht of approximately 15 per cent.

Be cause of an error in polarity, the oscillograms in the previous report[1] actually described the left-handed rotating region where an outward radial E field is required under the assumption of an E X B drift.

A perturbation of the plasma column can arise perpendicular to the field so that the plasma is shaped into a fluted column with an mθ dependence, where m gives the number of such flutes.[5] The present plasma has such a flute perturbation with the troughs extending into the luminous core of the discharge. No spiraling effect of the flute could be found along the axial direction.[6] Neither was such an effect found along a radial vector; in a two-probe system (separation of probe tips fixed at 3/4 inch) no phase change was found along a radial vector except between the opposite sides of the boundary of the luminous plasma core where the current to the outermost probe lagged by approximately $\pi/2$.

Figure IX-9 is another plot for the low B-field region where a mode change occurred even in the left-handed region. The signal was too erratic, however, for an accurate determination of the mode number just before crossover.

The two rotating regions have opposite dependence on mirror ratio as indicated in Fig. IX-10, in which, for two subcritical field values, the frequency shows no dependence on the mirror ratio and the rotation remains left-handed. Once the critical field
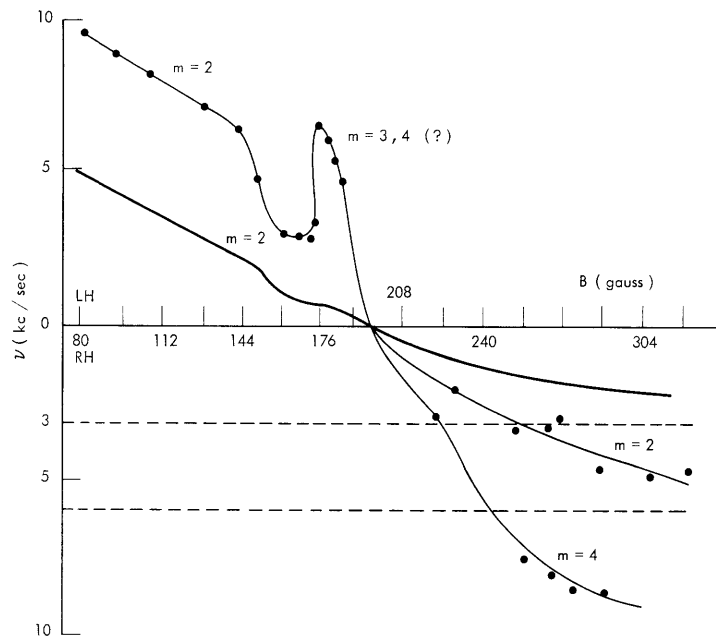
Fig. IX-9. Frequency and mode dependence of rotation on central magnetic field. Mirror ratio, 2.18; gun voltage, 820; pressure, 1.2×10^{-4} mm; cross-over, ≈ 210 gauss.
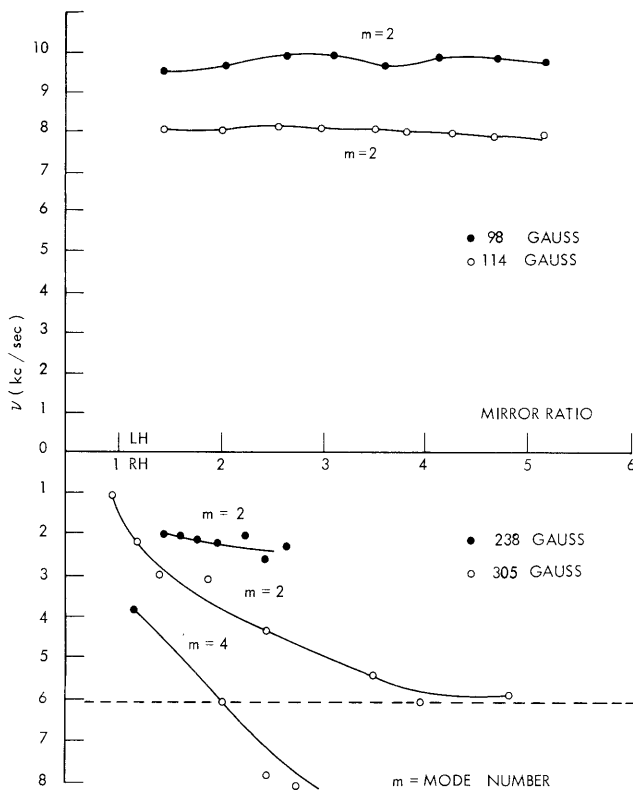

Fig. IX-10.

Dependence of rotation frequency on mirror ratio at constant central magnetic field.

is exceeded, the rotation remains right-handed; but here the frequency can be changed by varying the mirror ratio. Rotation was detected by a photomultiplier and by a wide variety of resistor grounded probes (Langmuir, antenna-type, and large geometrically fixed plates tangent to the chamber wall), biased or unbiased.

3. Probe Measurements

The luminous core of the discharge varies with the central field with a slight dependence on the mirror ratio, being approximately 1 inch in diameter at 200 gauss, and 1/4 inch at 400 gauss for a mirror ratio of 2. Particularly, the region from the luminous boundary to the chamber wall was investigated with a Langmuir probe. The average electron energy $\mathscr{E} = e\left[-V_p + \frac{3}{2} T_e \right]$ (where V_p and T_e are the space potential and electron temperature averaged over the azimuthal direction for some particular radial position) was found to be a constant through this region, and $\mathscr{E}$ changed only with changes of pressure, magnetic field, mirror ratio or gun voltage.

Experimental evidence indicates that the rotational reversal is associated with a reversal of the radial E field, and the direction is consistent with an E × B drift. The rotation reverses with a reversal of the axial B field. A Langmuir probe measured average plasma parameters along a radius at 1/2 inch intervals with a condenser used in the probe circuit to average azimuthal fluctuations caused by the perturbed plasma boundary. Such probe measurements were most reliable in the range below the critical magnetic field where the rotation was always left-handed and the plasma density outside the luminous core was $\approx 5 \times 10^9$/cc. (The density tripled when the gun voltage was raised from 800 v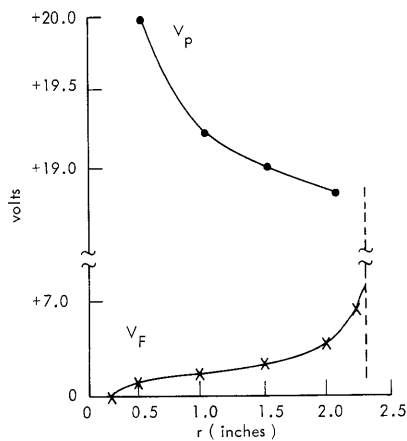olts to 1400 volts.) The subcritical field extended from ≈ 80 gauss to ≈ 200 gauss. A radially outward E field was found in this region to be approximately 60 volts/m just outside the luminous core boundary and approximately 10 volts/m near the cylindrical wall. The radial E field did not change significantly as the B field was increased; this indicates that the frequency followed an E/B dependence. If the rotational frequency based on E × B were calculated for the field just outside the luminous core, the calculated frequency would be almost an order of magnitude higher than the observed frequency. Under the assumption that the ion temperature is 0.1 ev, the inclusion of the ion pressure term[7] gives a further, but small

Fig. IX-11. An average plasma and floating potential plot.

contribution to the left-handed rotation.

For this plasma the radial electric field cannot be estimated from the easily obtainable floating potential, since the space and floating potentials were found to have opposite gradients in the region of interest. Radial temperature and density gradients were present with the average electron temperature ordinarily falling from 4 volts near the luminous boundary to 2 volts near the chamber wall, and the average density decreasing exponentially by a factor of three over this distance. Figure IX-11 is a typical average space potential V_p plot from which the radial E field is estimated, and the floating potential V_F for a subcritical magnetic field is given. The azimuthal fluctuations were very pronounced when V_F maintained an almost constant value along a radial vector. For subcritical fields, the plasma density remained at a rather constant value at some particular radial distance in the region outside the luminous core. But, as this value was exceeded, the density for some fixed radial position decreased linearly with the magnetic field, and the ion current to the chamber wall rapidly declined (see Fig. IX-12). Probe measurements thus became less reliable for estimating the space potential, especially at larger radial distances for fields above the critical field, but they did indicate that a
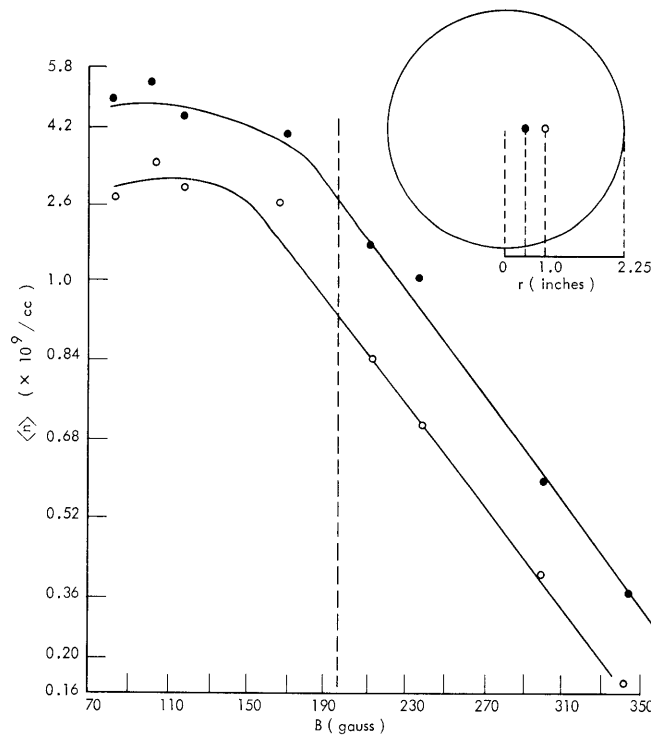

Fig. IX-12. Decrease of plasma density with increasing magnetic field at two fixed radial positions. Gun voltage, 800; mirror ratio, 2.1.
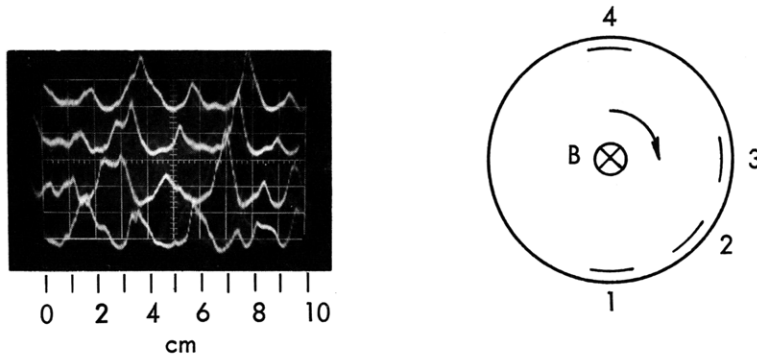
Fig. IX-13. Current-phase relations illustrating right-handed rotation. Magnetic field, 402 gauss; mirror ratio, 4.

reversal of the radial E field occurred at the rotational reversal.

Figure IX-12 indicates the type of response in the right-handed rotating region. Here the mode is M = 2, and the frequency 1.7 kc/sec. Inasmuch as the density in the region outside the luminous core is now only approximately 10^8/cc, the probes are biased at +22 volts, because of the low gain of the four-trace preamplifier units. For this oscillogram the current to the wall was sampled by a system of copper plates, 3/4 inch square, tangent to the chamber wall and grounded through resistors. The plate positions are indicated in Fig. IX-13, and the numbers refer to the corresponding traces (upper trace is number 1). Positive current reads upward.

4. Radial Ion Flow

The discharge is characterized by ion flow to the chamber wall with an associated increase of electron current along the discharge axis. There is some indication, though inconclusive, that the radial flow is by ordinary diffusion. With a condition that the conductivity across the magnetic field is negligible in the axial rate, the diffusion equation is solved for the steady-state, low-pressure plasma, and the radial dependence of the density is predicted[8] as

$$n(r) \approx K(r/q),$$

where K is a Hankel function, and q is the e-folding density length. With the assumptions used, the expression for q is

$$q = \frac{Lr_{ic}}{\pi\lambda_i},$$

where L is the interaction length, r_{ic} is the ion Larmor radius, and λ_i is the ion mean-free path. Experimentally, the average density in the region outside the luminous core is exponential as predicted. The calculated value of q is approximately 1 cm, a

reasonable value for the plasma.

For the present apparatus, with interaction length L = 70 cm, argon pressure 1.2×10^{-4} mm, B = 160 gauss, electron temperature 4 ev, and with the assumption that the ion temperature is 0.1 ev, the relation $\lambda_i < L < \lambda_e$, where λ_e is the electron mean-free path, holds; however, $L/\lambda_i \approx 2$, and $R/r_{ic} \approx 4$ with R = 5 cm, the radial plasma distance. These ratios are rather small for determining whether a collision-dominated diffusion is present.

Ordinary radial diffusion as determined by the ion diffusion coefficient may be expected from a "short-circuiting" mechanism,[9] whereby large radial E fields are prevented by the grounding of chamber and end walls as in the present apparatus. A rather large radial E field is present, however, and the short-circuiting effect may be inhibited by an end-wall potential sheath, as the space potential is high ($\approx$+20 volts).

J. K. Domen

References

1. J. K. Domen, "Steady-State Beam Plasma Discharge," Quarterly Progress Report No. 75, Research Laboratory of Electronics, M.I.T., October 15, 1964, pp. 51-54.

2. W. D. Getty and L. D. Smullin, J. Appl. Phys. **34**, 3421 (1963).

3. W. Bernstein, et al., Phys. Fluids **3**, 1019 (1960);
   N. Rostoker and A. C. Kolb, Phys. Rev. **124**, 965 (1961);
   N. D'Angelo and R. W. Motley, Phys. Fluids **6**, 422 (1963);
   H. Bodin and A. Newton, Phys. Fluids **6**, 1338 (1963);
   K. Bol, Phys. Fluids **7**, 1855 (1964);
   B. Hartenbaum, Ph.D. Thesis, Department of Mechanical Engineering, M.I.T., 1964;
   H. Lashinsky, Phys. Rev. Letters **12**, 121 (1964);
   K. I. Thomassen, Phys. Rev. Letters **14**, 587 (1965);
   D. L. Morse, Phys. Fluids **8**, 516 (1965).

4. W. A. Perkins and R. F. Post, Phys. Fluids **6**, 1537 (1963).

5. M. N. Rosenbluth and C. L. Longmire, Ann. Phys. **1**, 120 (1957); W. A. Perkins and R. F. Post, Phys. Fluids **6**, 1537 (1963).

6. B. B. Kadomtsev and A. V. Nedospasov, J. Nucl. Energy Part C **1**, 230 (1960).

7. L. Spitzer, Jr., Physics of Fully Ionized Gases (Interscience Publishers, Inc., New York, 1962), p. 31.

8. G. Guest and A. Simon, Phys. Fluids **5**, 503 (1962).

9. A. Simon, Phys. Rev. **98**, 317 (1955); F. Boeschoten and F. Schwirzke, Nuclear Fusion **2**, 54 (1962); F. Boeschoten, J. Nucl. Energy Part C **6**, 339 (1964).